ORIGINAL ARTICLE

Development of sliding mode control based on diagonal recurrent neural network for coupled tank system

Ahmad M. El-Nagar[1] · Mohamed I. Abdo[1]

Abstract

This study presents the development of sliding mode control (SMC) using the diagonal recurrent neural network (DRNN) for nonlinear systems. Firstly, the SMC for linear systems is developed for nonlinear coupled tank system. Second, the DRNN is used to design the equivalent part of the SMC law, which is performed to approximate the dynamics of a controlled process. Third, the sliding surface for the switching control is developed using the DRNN. The DRNN parameters are tuned using Lyapunov function to achieve the controlled process stability. For the developed scheme, discontinuous signum function is used to compensate the chattering phenomenon. The developed scheme is applied for controlling the uncertain nonlinear coupled tank system. The simulation results indicate that the developed scheme can respond to the effects of system uncertainties compared to other existing schemes.

Keywords Sliding mode control · Diagonal recurrent neural network · Sliding surface · Coupled tank system · Lyapunov function

1 Introduction

Most practical dynamic systems have uncertain effects such as parameter uncertainties, external disturbances, model nonlinearities and structure uncertainties. These challenging problems cannot be covered using linear and conventional controllers. Subsequently, it is essential to develop robust control schemes for solving such problems and to obtain certain performance requirements [1–3]. In recent years, robust adaptive schemes based on trajectory tracking have attracted great attention for nonlinear systems such as adaptive probabilistic Takagi–Sugeno–Kang (TSK) fuzzy controller [4], adaptive interval type-2 TSK fuzzy controller [5], adaptive sliding mode control (SMC) [6] and SMC based on proportional-integral-derivative (PID) and proportional-integral (PI) sliding surface, respectively [7, 8].

SMC approach is a class of the variable structure control schemes, which is a nonlinear robust controller that is able to respond insensitivity to structure uncertainties, rejection of an external disturbance, fast and good transient response, and stable control system [9]. SMC contains a switching control law that moves the states of the plant from any initial value on the sliding surface, which is set by the user in the switching surface and to preserve the system states on a desired sliding surface [10, 11]. However, the SMC includes the following problems: (1) it is necessary to obtain the precise mathematical model for the controlled process to design the SMC [9]. This problem decreases the performance of the controller in some control applications. (2) chattering phenomenon, which is an inherent problem in the design of SMC [10]. This problem also decreases the SMC performance. (3) uncertainty bounds, which are required for designing the switching control law of SMC [11]. To avoid such problems, several researchers proposed several approaches for solving the chattering problems such as approximating the discontinuous switching control law by using saturation function [12], using low pass filter [13], using variable structure adaptive control [14] and

✉ Ahmad M. El-Nagar
ahmed.elnagar@el-eng.menofia.edu.eg

Mohamed I. Abdo
mohamed.abdelrahman@el-eng.menofia.edu.eg

[1] Department of Industrial Electronics and Control Engineering, Faculty of Electronic Engineering, Menoufia University, Menof 32852, Egypt

using adaptive intelligent technique [15]. On the other hand, some researchers used the adaptive control schemes using Lyapunov theory such as genetic algorithm [16], event-triggering dissipative control [17] and other schemes for complex industrial systems [18] to handle the problem of knowing the perfect mathematical model of the controlled process. In [19], SMC with a bound estimation was introduced for controlling robot manipulator to solve the problem of the uncertainty bounds.

In recent years, several researchers have integrated the SMC with intelligent techniques such as fuzzy logic systems (FLSs) [20] and neural networks (NNs) [9, 11, 21–29]. In [10], the fuzzy SMC with PI sliding surface for linear system was introduced. SMC law requires a precise knowledge about the controlled process. Moreover, the FLS was proposed to compensate the chattering phenomenon. In [9], an adaptive radial basis function NN (RBFNN)-based SMC for nonlinear plants was introduced. RBFNN was performed to approximate the unknown parameters of the controlled process. Also, the problem of chattering is solved based on a smooth continuous control action. In [11], a NN-based SMC for rotating stall and surge in axial compressors was introduced. The adaptive NN was used to avoid the problem of obtaining a precise mathematical model for the controlled process. In [25], a recurrent NN (RNN) based fuzzy SMC was introduced for 4-degree freedom remotely operated vehicle. The model uncertainties were compensated and estimated using RNN. On the other hand, the chattering phenomenon was handled using FLS as a switching term. In [29], NN was proposed to approximate the unknown continuous uncertainties and disturbance for an autonomous surface vehicle where the uncertainty bounds for the sliding surface was compensated using Lyapunov theory.

1.1 Motivation

In this paper, SMC based on diagonal RNN (DRNN) is introduced for uncertain nonlinear systems. The developed controller is motivated from the previous published works in [9–11, 21–29] to cover the disadvantages of the work in [10]. First, the SMC in [10], which was designed to linear systems is developed to uncertain nonlinear system (coupled tank system as a benchmark in this paper). Second, the NN in [9, 11, 21–29], which was used to approximate the unknown controlled system is developed to DRNN as the first time that used with SMC based on the authors' best knowledge. DRNN is a type of NN, which belongs to the partially connected RNNs [30]. DRNN was introduced to identify nonlinear systems, which have a superior modeling accuracy compared with other NN techniques [31].

In this paper, the SMC is designed based on the DRNN. The SMC law consists of two terms; the first one is the equivalent control law, which is performed based on the DRNN. The nonlinear controlled system is approximated using DRNN. The second part is the switching control signal, which is dependent on the sliding surface. The sliding surface is performed based on DRNN. For the proposed controller, the discontinuous signum function is used to compensate the chattering problem. The updating weights of DRNN are obtained using Lyapunov function to guarantee the controlled system stability. The proposed scheme is designed for controlling uncertain nonlinear coupled tank system. The simulation results indicate that the developed controller can respond to the effects of system uncertainties and external disturbances compared to other existing schemes.

1.2 Novelties and contributions

The main contributions of this study are summarized as:

1. Design a novel SMC based on the DRNN for nonlinear systems that is motivated from previous works.
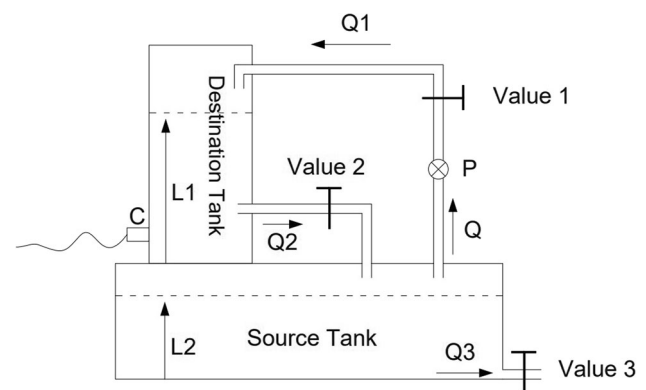
Table 1 Parameters of coupled tank system [32]

A_d	Destination tank area	0.03 m^2
A_s	Source tank area	0.08 m^2
C_1	Controlled cross section of valve 1	0.00008 m^2
C_2	Controlled cross section of valve 2	0.00008 m^2
C_3	Controlled cross section of valve 3	0.00008 m^2
D_1	Discharge coefficient	1
D_2	Discharge coefficient	1
D_3	Discharge coefficient	1
L_1	Destination tank level	0.6 m
L_2	Source tank level	0.2 m
u	Input voltage	12 v
K_g	Pump gain	7.5 m^3/s.v
K_t	Transducer gain	40 v/m
g	Gravity constant	9.8 m/s

Fig. 1 Coupled tank system [32]

2. Developing the sliding surface based on DRNN.
3. Updating the DRNN weights using Lyapunov function to achieve the controlled system stability.
4. The problem of the knowledge of the controlled system and chattering phenomenon are compensated.

The remainder of this paper is organized as: Sect. 2 presents the problem formulation. The second order SMC for nonlinear coupled tank system is introduced in Sect. 2. The proposed SMC based on the DRNN is presented in Sect. 3. The updating algorithm for the DRNN parameters using Lyapunov function is presented in Sect. 4. Simulation results for the coupled tank system is presented in Sect. 5. Finally, conclusions are given in Sect. 6.

2 Problem formulation

Figure 1 shows the coupled tank system, which is used in this paper as a benchmark. It is considered as one of the hydraulic control systems in industrial applications [32, 33]. The function of the controller is controlling the destination tank level (L_1) by varying the pump (P) flow using valve 1 or by valve 2, which is considered as a disturbance.

The relation between the pump supply voltage (u) and the input flow (Q) is given as [32]:

$$\begin{cases} Q = K_g u \\ Q_2 = C_2 D_2 \sqrt{2g(L_1 - L_2)} \\ Q_3 = C_3 D_3 \sqrt{2gL_2} \end{cases} \quad (1)$$

The destination tank can be filled from the source tank by opening the valve 1 placed after the pump, which changes the incoming flow. The output flow (Q_2) can change using valve 2, which inserted below the destination tank. Consider $Q_1 = Q$ for the level control case, we obtain the following using the flow equilibrium equation [32]:

$$\begin{cases} \dot{L}_1 = \frac{1}{A_d}(Q_1 - Q_2) \\ \dot{L}_2 = \frac{1}{A_s}(Q_2 - Q_3) \end{cases} \quad (2)$$

Finally, the mathematical model of the coupled tank system is given as [32]:

$$\begin{cases} \dot{L}_1 = \frac{1}{A_d}(K_g u - C_2 D_2 \sqrt{2g(L_1 - L_2)}) \\ \dot{L}_2 = \frac{1}{A_s}(C_2 D_2 \sqrt{2g(L_1 - L_2)} - C_3 D_3 \sqrt{2gL_2}) \\ y = K_t L_1 \end{cases} \quad (3)$$

The above equation can be rewritten as the following considering $x_a = (0pt x_{a1} x_{a2})$, $x_{a1} = L_1$ and $x_{a2} = L_2$

$$\begin{cases} \dot{x}_{a1} = \frac{1}{A_d}(K_g u - C_2 D_2 \sqrt{2g(x_{a1} - x_{a2})}) \\ \dot{x}_{a2} = \frac{1}{A_s}(C_2 D_2 \sqrt{2g(x_{a1} - x_{a2})} - C_3 D_3 \sqrt{2gx_{a2}}) \\ y = K_t x_{a1} \end{cases} \quad (4)$$

Using the above equation, the nonlinear model of the coupled tank system is obtained as:

$$\begin{cases} \dot{x}_{a1} = f_1(x_a) + Bu \\ \dot{x}_{a2} = f_2(x_a) \\ y = C x_{a1} \end{cases} \quad (5)$$

where

$f_1(x_a) = \frac{-C_2 D_2}{A_d} \sqrt{2g(x_{a1} - x_{a2})}$, $C = K_t$, $f_2(x_a) = \frac{C_2 D_2}{A_s} \sqrt{2g(x_{a1} - x_{a2})} - \frac{C_3 D_3}{A_s} \sqrt{2gx_{a2}}$ and $B = \frac{K_g}{A_d}$.

The nonlinear model, which is described in Eq. (5), can be modified by considering parameter uncertainties. Therefore, the nonlinear model is given as:

$$\begin{cases} \dot{x}_{a1} = f_{1n}(x_a) + \Delta f_1(x_a) + Bu + E_1(t) \\ \dot{x}_{a2} = f_{2n}(x_a) + \Delta f_2(x_a) + E_2(t) \\ y = C x_{a1} \end{cases} \quad (6)$$

where $f_{1n}(x_a), f_{2n}(x_a)$ represent the nominal values of the nonlinear functions; $f_1(x_a)$ and $f_2(x_a)$, respectively. $\Delta f_1(x_a)$ and $\Delta f_2(x_a)$ represent the parameter uncertainties of the nonlinear functions $f_1(x_a)$ and $f_2(x_a)$, respectively. $E_1(t)$ and $E_2(t)$ represent the unknown external perturbations. It is assumed that all the uncertainties can be given as:

$$\begin{cases} \rho_1(t) = \Delta f_1(x_a) + E_1(t) \\ \rho_2(t) = \Delta f_2(x_a) + E_2(t) \end{cases} \quad (7)$$

Therefore, Eq. (6) can be rewritten as:

$$\begin{cases} \dot{x}_{a1} = f_{1n}(x_a) + Bu + \rho_1(t) \\ \dot{x}_{a2} = f_{2n}(x_a) + \rho_2(t) \\ y = C x_{a1} \end{cases} \quad (8)$$

3 Second order sliding mode control

In this section, the second order SMC (SOSMC), which is applied previously [8, 10], is developed to applied to uncertain nonlinear coupled tank system as described in Eq. (8). The PI sliding surface is chosen as [10]:

$$S(t) = k_1 e(t) + k_2 \int_0^t e(\tau) d\tau \quad (9)$$

where $e(t) = x_{d1} - x_{a1}$ is the tracking error, x_{d1} is the desired level and x_{a1} is the actual level of the coupled tank system defined by Eq. (8). The parameters; k_1 and k_2 are the proportional and integral positive gains, respectively for the PI sliding surface.

The main goal of the SOSMC is to make the output of the system; x_{a1} to successfully track a given desired signal; x_{d1} under the effect of system uncertainties. Therefore, the sliding surface; $S(t)$ and the time derivative of the sliding surface; $\dot{S}(t)$ should equal zero to make the tracking error kept on the sliding surface [10]. The total control law of the SOSMC consists of two parts, which is given in Eq. (10); the first is the equivalent control term; $u_{eq}(t)$ and the other is the switching control term; $u_{sw}(t)$.

$$u(t) = u_{eq}(t) + u_{sw}(t) \qquad (10)$$

The equivalent control term; $u_{eq}(t)$ is obtained as the solution of $\dot{S}(t) = 0$ under nominal system dynamic model ($\rho_1(t) = \rho_2(t) = 0$). The time derivative of sliding surface, which is described in Eq. (9) is obtained as:

$$\dot{S}(t) = k_1\dot{e}(t) + k_2 e(t) \qquad (11)$$

Putting $e(t) = x_{d1} - x_{a1}$ and $\dot{e}(t) = \dot{x}_{d1} - \dot{x}_{a1}$, Eq. (11) can be rewritten as:

$$\dot{S}(t) = k_1\dot{x}_{d1} - k_1\dot{x}_{a1} + k_2 x_{d1} - k_2 x_{a1} \qquad (12)$$

Substitute $\dot{x}_{a1}$ from Eq. (8) into Eq. (12), we get the following:

$$\dot{S}(t) = k_1\dot{x}_{d1} + k_2 x_{d1} - k_2 x_{a1} - k_1 f_{1n}(x_a) - k_1 Bu - k_1\rho_1(t) \qquad (13)$$

Putting $\dot{S}(t) = 0$ and $\rho_1(t) = 0$, the equivalent control term; $u_{eq}(t)$ is obtained as:

$$u_{eq}(t) = \frac{1}{k_1 B}[k_1\dot{x}_{d1} + k_2 e(t) - k_1 f_{1n}(x_a)] \qquad (14)$$

The above equation shows $u_{eq}(t)$, which provides the desired performance for the controlled system. The switching control term; $u_{sw}(t)$ should be obtained to compensate the effect of the system uncertainties such as external disturbances and parameters variations. Lyapunov function; $V(t)$ is chosen to design the switching control term; $u_{sw}(t)$ as follow:

$$V(t) = \frac{1}{2}S^2(t) \qquad (15)$$

The time derivative $\dot{V}(t)$ is obtained as:

$$\dot{V}(t) = S(t)\dot{S}(t) \qquad (16)$$

By Substituting Eqs. (10 and 13) into Eq. (16), we get the following:

$$\dot{V}(t) = S(t)[k_1\dot{x}_{d1} + k_2 x_{d1} - k_2 x_{a1} - k_1 f_{1n}(x_a) - k_1 B(u_{eq} + u_{sw}) - k_1\rho_1(t)] \qquad (17)$$

By Substituting Eq. (14) into Eq. (17), we get the following:

$$\dot{V}(t) = S(t)\Big[k_1\dot{x}_{d1} + k_2 x_{d1} - k_2\, x_{a1} - k_1 f_{1n}(x_a) \\ -k_1 B\Big(\frac{1}{k_1 B}(k_1\dot{x}_{d1} + k_2 e(t) - k_1 f_{1n}(x_a))\Big) - k_1 B u_{sw} - k_1\rho_1(t)\Big] \qquad (18)$$

The above equation can be rearranged as:

$$\dot{V}(t) = S(t)[k_1\dot{x}_{d1} + k_2 e(t) - k_1 f_{1n}(x_a) - k_1\dot{x}_{d1} - k_2 e(t) \\ + k_1 f_{1n}(x_a) - k_1 B u_{sw} - k_1\rho_1(t)] \\ = S(t)[-k_1 B u_{sw} - k_1\rho_1(t)] \qquad (19)$$

The switching control signal; $u_{sw}(t)$ can be selected as:

$$u_{sw}(t) = \frac{-k_r}{k_1 B}sign(S(t)) \qquad (20)$$

where k_r is the switching control gain and $sign(\cdot)$ denotes sign function that defined as [10]:

$$sign(S(t)) = \begin{cases} 1, S(t) > 0 \\ 0, S(t) = 0 \\ -1, S(t) < 0 \end{cases} \qquad (21)$$

By Substituting Eq. (20) into Eq. (19), we get the following:

$$\dot{V}(t) = k_r S(t)sign(S(t)) - k_1 S(t)\rho_1(t) \qquad (22)$$

By using $|S(t)| = S(t)sign(S(t))$, the above equation is rewritten as:

$$\dot{V}(t) = k_r|S(t)| - k_1 S(t)\rho_1(t) \qquad (23)$$

$$\dot{V}(t) \leq -|S(t)|(-k_r + k_1\rho_{max}(t)) \qquad (24)$$

To achieve controlled system stability using SOSMC and the reaching condition $\dot{V}(t) < 0$ is satisfied, the switching control gain; k_r must be selected as:

$$k_r < k_1\rho_{max}(t) \qquad (25)$$

Therefore, the total control law of the SOSMC is given as:

$$u(t) = \frac{1}{k_1 B}[k_1\dot{x}_{d1} + k_2 e(t) - k_1 f_{1n}(x_a) - k_r sign(S(t))] \qquad (26)$$
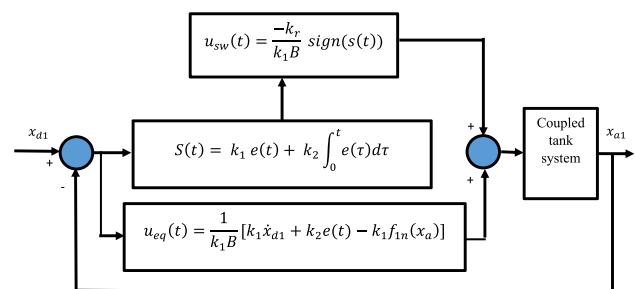

Fig. 2 Block diagram of SOSMC for coupled tank system

The block diagram of the SOSMC scheme is shown in Fig. 2. The SOSMC law that is given in Eq. (26) can compensate the chattering problem where the switching control part contains the discontinuous signum function. Moreover, the witching control gain; k_r is concerned with the boundaries of unknown uncertainties (as indicated by the stability condition in Eq. (25)), and it is required to know the precise mathematical model of the controlled uncertain system as it appears in the control signal.

4 SMC based on diagonal recurrent NN

In this section, the structure of DRNN is presented. Then, the development of SMC based on DRNN is introduced.

4.1 Structure of DRNN

The structure of the DRNN is shown in Fig. 3. It consists of three layers; input layer, hidden layer, and output layer [30]. The input vector for the DRNN is $\mathbf{Z}(t) = [z_1(t)z_2(t) \cdots z_P(t)]^T$, the hidden weight matrix for the hidden layer is represented by Eq. (27) and the diagonal weight vector for the hidden nodes is represented as $\mathbf{W^D} = [w_1^D w_2^D \cdots w_R^D]^T$. The output weight vector for the output layer is represented as $\mathbf{W^O} = [w_1^O w_2^O \cdots w_R^O]^T$. P and R denote the number of inputs and the number of nodes in hidden layer, respectively.

$$W^I = \begin{bmatrix} w_{11}^I & \cdots & w_{1P}^I \\ \vdots & \ddots & \vdots \\ w_{R1}^I & \cdots & w_{RP}^I \end{bmatrix} \qquad (27)$$

For any recurrent neuron, the output $m_r(t)$ at any t time and sampling period T is obtained as follows:

$$g_r(t) = \sum_{p=1}^{P} w_{rp}^I z_p(t) + w_r^D(t)m_r(t-T), r = 1, 2, \ldots R \text{ and } P$$
$$= 1, 2, \ldots P \qquad (28)$$

$$m_r(t) = f(g_r(t)) = \frac{2}{1 + e^{-\sigma g_r(t)}} - 1,, r = 1, 2, \ldots R \qquad (29)$$

where σ is constant. The DRNN output; $O_{DRNN}(t)$ is given as:

$$O_{DRNN}(t) = \sum_{r=1}^{R} w_r^O(t)m_r(t) = \mathbf{W^O}(t)\mathbf{M}(t) \qquad (30)$$

where $(t) = [m_1(t)m_2(t) \cdots m_R(t)]^T$.

4.2 Proposed structure

The approximation ability of the DRNN is used to propose the SMC based on DRNN (SMC-DRNN), where the equivalent control term of SMC law, which depends on the dynamic model of a controlled system, is approximated using DRNN. Equation (13) can be rearranged as follows:

$$\dot{S}(t) = k_1 \dot{x}_{d1} + k_2 e(t) - k_1 f_{1n}(x_a) - k_1 Bu(t) - k_1 \rho_1(t) \qquad (31)$$

$$\dot{S}(t) = -k_1 Bu - k_1 \rho_1(t) + f_d(\mathbf{x}_A) \qquad (32)$$

where $f_d(\mathbf{x}_A)$ represents an unknown uncertain nonlinear function and is defined as:

Fig. 3 Structure of DRNN
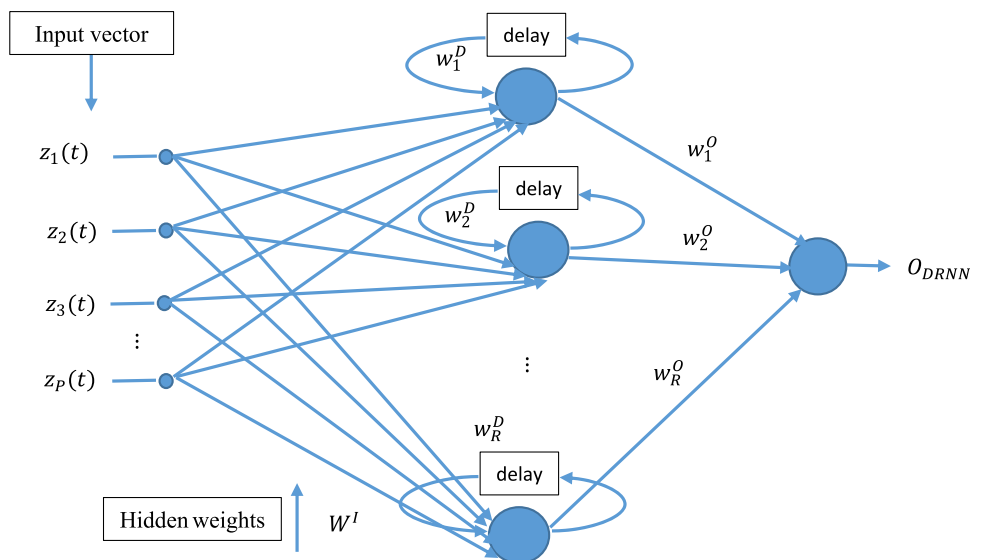
$$f_d(\boldsymbol{x}_A) = k_1\dot{x}_{d1} + k_2e(t) - k_1f_{1n}(x_a) \tag{33}$$

where $\boldsymbol{x}_A = [e(t)\dot{x}_{d1}(t)x_{a1}(t)x_{a2}(t)]^T$. The function; $f_d(\boldsymbol{x}_A)$ can be universally approximated using the DRNN as:

$$f_d(\boldsymbol{x}_A) = \boldsymbol{W}_d^O(t)\boldsymbol{M}_d(t) \tag{34}$$

where $\boldsymbol{W}_d^O(t) = \left[w_{d1}^O(t)w_{d2}^O(t)\cdots w_{dR}^O(t)\right]^T$ is the output weight vector of the DRNN, which approximate the function; $f_d(\boldsymbol{x}_A)$ and $\boldsymbol{M}_d(t) = [m_{d1}(t)m_{d2}(t)\cdots m_{dR}(t)]^T$ is the input vector for the output layer and it is obtained as the following where R is the number of nodes in hidden layer of DRNN, which approximate the function; $f_d(\boldsymbol{x}_A)$:

$$\boldsymbol{M}_d(t) = f[\boldsymbol{G}_d(t)] \tag{35}$$

$$\boldsymbol{G}_d(t) = \boldsymbol{W}_d^D(t)\boldsymbol{M}_d(t-T) + \boldsymbol{W}_d^I(t)\boldsymbol{x}_A \tag{36}$$

where $\boldsymbol{W}_d^D(t) = \left[w_{d1}^D w_{d2}^D \cdots w_{dR}^D\right]^T$ is the diagonal weight vector for the hidden layer of DRNN, which approximate the function; $f_d(\boldsymbol{x}_A)$ and $\boldsymbol{W}_d^I$ is the weight matrix for the hidden layer of DRNN, which is given as:

$$\boldsymbol{W}_d^I(t) = \begin{bmatrix} w_{d11}^I & w_{d12}^I & w_{d13}^I & w_{d14}^I \\ \vdots & \vdots & \vdots & \vdots \\ w_{dR1}^I & w_{dR2}^I & w_{dR3}^I & w_{dR4}^I \end{bmatrix} \tag{37}$$

Therefore, the equivalent control part; $u_{eq-DRNN}(t)$ for the proposed SMC-DRNN is obtained as the following by substituting Eqs. (34–36) into Eq. (14):

$$u_{eq-DRNN}(t) = \frac{1}{k_1B}[f_d(\boldsymbol{x}_A)] = \frac{1}{k_1B}\left[\boldsymbol{W}_d^O(t)\boldsymbol{M}_d(t)\right] \tag{38}$$

$$u_{eq-DRNN}(t) = \frac{1}{k_1B}\left[\boldsymbol{W}_d^O(t)f\left[\boldsymbol{W}_d^D(t)\boldsymbol{M}_d(t-T) + \boldsymbol{W}_d^I(t)\boldsymbol{x}_A\right]\right] \tag{39}$$

On the other hand, the switching control part for the proposed SMC-DRNN is developed, where the function of the sliding surface; $S(t)$ is designed based on DRNN. Therefore, the proposed sliding surface; $S_{DRNN}(t)$ is obtained as follows:

$$S_{DRNN}(t) = \boldsymbol{W}_s^O(t)f[\boldsymbol{W}_s^D(t)\boldsymbol{M}_s(t-T) + \boldsymbol{W}_s^I(t)\boldsymbol{x}_s] \tag{40}$$

where $\boldsymbol{W}_s^O(t) = \left[w_{s1}^O(t)w_{s2}^O(t)\cdots w_{sM}^O(t)\right]^T$ is the output weight vector of the DRNN, which approximate the sliding surface; $S_{DRNN}(t)$ and $\boldsymbol{M}_s(t) = [m_{s1}(t)m_{s2}(t)\cdots m_{sD}(t)]^T$ is the input vector for the output layer where D is the number of nodes in hidden layer of DRNN, which approximate the sliding surface; $S_{DRNN}(t)$. $\boldsymbol{x}_s = [e(t)\int e(t)]^T$ is the input vector, $\boldsymbol{W}_s^D(t) = \left[w_{s1}^D w_{s2}^D \cdots w_{sD}^D\right]^T$ is the diagonal weight vector for the hidden layer of DRNN, which approximate the sliding surface; $S_{DRNN}(t)$ and $\boldsymbol{W}_s^I$ is the weight matrix for the hidden layer of DRNN, which is given as:

$$\boldsymbol{W}_d^I(t) = \begin{bmatrix} w_{s11}^I & w_{s12}^I \\ \vdots & \vdots \\ w_{sD1}^I & w_{sD2}^I \end{bmatrix} \tag{41}$$

Therefore, the switching control term for the proposed SMC-DRNN; $u_{sw-DRNN}(t)$ is obtained as follows:

$$u_{sw-DRNN}(t) = \frac{-k_r}{k_1B}sign(S_{DRNN}(t)) \tag{42}$$

$$u_{sw-DRNN}(t) = \frac{-k_r}{k_1B}sign\left(\boldsymbol{W}_s^O(t)f\left[\boldsymbol{W}_s^D(t)\boldsymbol{M}_s(t-T) + \boldsymbol{W}_s^I(t)\boldsymbol{x}_s\right]\right) \tag{43}$$

Therefore, the total control law of the proposed SMC-DRNN is given as:

$$u_{DRNN}(t) = \frac{1}{k_1B}\Big[\boldsymbol{W}_d^O(t)f\left[\boldsymbol{W}_d^D(t)\boldsymbol{M}_d(t-T) + \boldsymbol{W}_d^I(t)\boldsymbol{x}_A\right] \\ -k_r\left(sign\left(\boldsymbol{W}_s^O(t)f\left[\boldsymbol{W}_s^D(t)\boldsymbol{M}_s(t-T) + \boldsymbol{W}_s^I(t)\boldsymbol{x}_s\right]\right)\right)\Big] \tag{44}$$

Figure 4 indicates the block diagram of the developed SMC-DRNN. The total control law of the proposed scheme; $u_{DRNN}(t)$ consists of two terms; the first term is the equivalent control term; $u_{eq-DRNN}(t)$, which performed using the DRNN to approximate the dynamics of the controlled system to compensate the problem of the precise knowledge of the mathematical model for the controlled process. The other part is the switching control term; $u_{sw-DRNN}(t)$, which depends on the sliding surface that designed based on the DRNN to compensate the problem of chattering. The weights of the DRNNs are tuned using the Lyapunov function to achieve the controlled system stability. In the next section, the updating algorithm is introduced in detail.

5 Updating algorithm based on Lyapunov function

In this section, the weights of the DRNN are updated online using Lyapunov function to achieve the coupled tank system stability. The weight vectors; $\boldsymbol{W}_d^I$, $\boldsymbol{W}_d^D$ and $\boldsymbol{W}_d^O$ for the DRNN, which approximate the equivalent control term and the weight vectors; $\boldsymbol{W}_s^I$, $\boldsymbol{W}_s^D$ and $\boldsymbol{W}_s^O$ for the DRNN, which approximate the sliding surface are updated online. The weight adjustment rule is derived using the Lyapunov stability criterion. The error at the ϱ th instant between the plant output; $x_{a1}(\varrho)$ and the reference input; $x_{d1}(\varrho)$ is referred to as $e(\varrho) = x_{d1}(\varrho) - x_{a1}(\varrho)$, which is utilized to adjust the weight vectors of the DRNN. The following is the derivation of the weight adjustment rule using the Lyapunov stability criteria:

Fig. 4 Block diagram of the proposed SMC-DRNN for coupled tank system
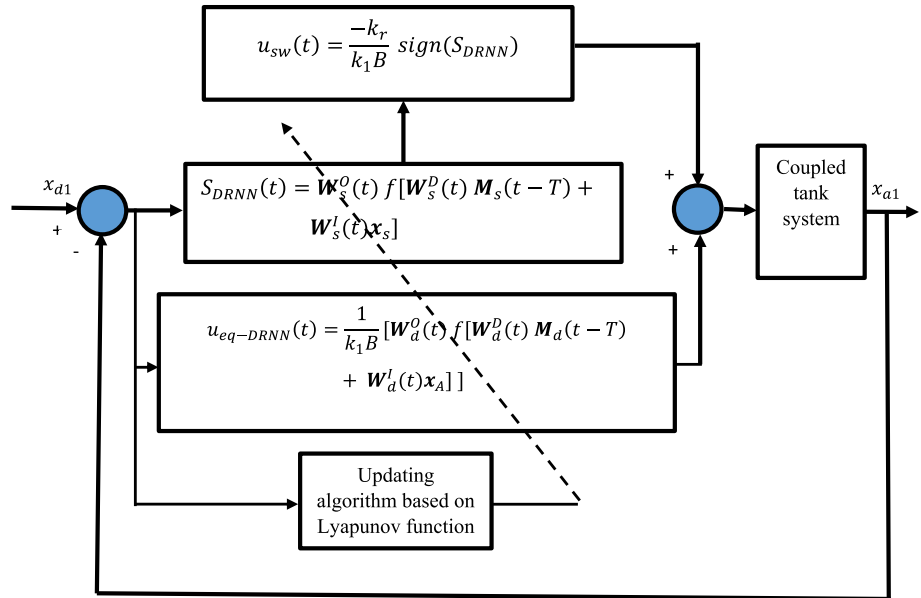
First, a scalar function; $V_L(X)$ should be selected, where X represents an argument vector, and $V_L(X)$ is positive definite for all initial conditions of its arguments, except when they are all simultaneously equal to zero [31]. A system is considered asymptotically stable if it satisfies both conditions described by Eqs. (45) and (46).

$$V_L(X) > 0 \, for \, all \, X \, except \, X = 0 \tag{45}$$

$$\frac{dV_L}{dt} = negative \, definite \, for \, all \, X \tag{46}$$

The controlled system is asymptotically stable if both conditions are satisfied. To establish the basis for the weight learning algorithm, we can express the generalized form of the weight update equation as follows:

$$\mathbb{N}(\varrho + 1) = \mathbb{N}(\varrho) - \eta \Delta \mathbb{N}(\varrho) \tag{47}$$

where $\mathbb{N}(\varrho)$ represents a generalized weight vector, which denotes ($W_d^I, W_d^D, W_d^O W_s^I, W_s^D$ and W_s^O). Here, $\Delta \mathbb{N}(\varrho)$ represents the necessary weight adjustment to be made and η represents the learning rate. Let $\varepsilon(\varrho)$ be the cost function, which is a function of the error; (ϱ). It is defined as:

$$\varepsilon(\varrho) = \frac{1}{2}(e(\varrho))^2 \tag{48}$$

The positive definite Lyapunov function is chosen as:

$$V_L(\varrho) = \frac{1}{2}[(e(\varrho))^2 + (\mathbb{N}(\varrho))^2] \tag{49}$$

The time derivative of $V_L(\varrho)$ in discrete form is determined as:

$$\Delta V_L(\varrho) = V_L(\varrho + 1) - V_L(\varrho) \le 0 \tag{50}$$

Theorem: *For Lyapunov function, $V_L(\varrho) = \frac{1}{2}[(e(\varrho))^2 + (\mathbb{N}(\varrho))^2] > 0$, condition $\Delta V_L(\varrho) = V_L(\varrho + 1) - V_L(\varrho) \le 0$ is satisfied if and only if*

$$\Delta \mathbb{N}(\varrho) = -\frac{\left\{ \mathbb{N}(\varrho) + e(\varrho)\left[\frac{\partial e(\varrho)}{\partial \mathbb{N}(\varrho)}\right] \right\}}{1 + \left[\frac{\partial e(\varrho)}{\partial \mathbb{N}(\varrho)}\right]^2} \tag{51}$$

Proof By substituting Eq. (49) into Eq. (50), we get the following:

$$\Delta V_L(\varrho) = \frac{1}{2}\{[(e(\varrho + 1))^2 + (\mathbb{N}(\varrho + 1))^2] - [(e(\varrho))^2 + (\mathbb{N}(\varrho))^2]\} \tag{52}$$

The above equation can be rearranged as:

$$\Delta V_L(\varrho) = \frac{1}{2}[(e(\varrho + 1))^2 - (e(\varrho))^2] + \frac{1}{2}[(\mathbb{N}(\varrho + 1))^2 - (\mathbb{N}(\varrho))^2] \tag{53}$$

$$\Delta V_L(\varrho) = \frac{1}{2}[e(\varrho + 1) + e(\varrho)][e(\varrho + 1) - e(\varrho)] + \frac{1}{2}[\mathbb{N}(\varrho + 1) + \mathbb{N}(\varrho)][\mathbb{N}(\varrho + 1) - \mathbb{N}(\varrho)] \tag{54}$$

Let $\Delta e(\varrho) = e(\varrho + 1) - e(\varrho)$ and $\Delta \mathbb{N}(\varrho) = \mathbb{N}(\varrho + 1) - \mathbb{N}(\varrho)$ and putting them in Eq. (54), we get the following:

$$\Delta V_L(\varrho) = \frac{1}{2}\{\Delta e(\varrho)[\Delta e(\varrho) + 2e(\varrho)] + \Delta \mathbb{N}(\varrho)[\Delta \mathbb{N}(\varrho) + 2\mathbb{N}(\varrho)]\} \tag{55}$$

The above equation can be written as:

$$\Delta V_L(\varrho) = \frac{1}{2}[\Delta\mathbb{N}(\varrho)]^2\left[1 + \left[\frac{\Delta e(\varrho)}{\Delta\mathbb{N}(\varrho)}\right]^2\right]$$
$$+ \Delta\mathbb{N}(\varrho)\left[\mathbb{N}(\varrho) + e(\varrho)\left[\frac{\Delta e(\varrho)}{\Delta\mathbb{N}(\varrho)}\right]\right] \quad (56)$$

For a very small change, Eq. (56) can be written as:

$$\Delta V_L(\varrho) = \frac{1}{2}[\Delta\mathbb{N}(\varrho)]^2\left[1 + \left[\frac{\partial e(\varrho)}{\partial\mathbb{N}(\varrho)}\right]^2\right]$$
$$+ \Delta\mathbb{N}(\varrho)\left[\mathbb{N}(\varrho) + e(\varrho)\left[\frac{\partial e(\varrho)}{\partial\mathbb{N}(\varrho)}\right]\right] \quad (57)$$

From the above equation, let the following:

$$\Delta V_L(\varrho) = \frac{1}{2}[\Delta\mathbb{N}(\varrho)]^2\left[1 + \left[\frac{\partial e(\varrho)}{\partial\mathbb{N}(\varrho)}\right]^2\right]$$
$$+ \Delta\mathbb{N}(\varrho)\left[\mathbb{N}(\varrho) + e(\varrho)\left[\frac{\partial e(\varrho)}{\partial\mathbb{N}(\varrho)}\right]\right]$$
$$= -\frac{\delta}{2} \quad (58)$$

where $\delta \geq 0$ in order to make $\Delta V_L(\varrho) \leq 0$. Therefore, the above equation becomes as:

$$\Delta V_L(\varrho) = \frac{1}{2}[\Delta\mathbb{N}(\varrho)]^2\left[1 + \left[\frac{\partial e(\varrho)}{\partial\mathbb{N}(\varrho)}\right]^2\right]$$
$$+ \Delta\mathbb{N}(\varrho)\left[\mathbb{N}(\varrho) + e(\varrho)\left[\frac{\partial e(\varrho)}{\partial\mathbb{N}(\varrho)}\right]\right] + \frac{\delta}{2}$$
$$= 0 \quad (59)$$

Consider a general quadratic equation: $az^2 + bz + c = 0$, then the roots of it are given by

$$r_1 = \frac{-b + \sqrt{b^2 - 4ac}}{2a} \text{ and } r_1 = \frac{-b - \sqrt{b^2 - 4ac}}{2a} \quad (60)$$

Comparing the general quadratic equation and Eq. (59), it can be seen that $\Delta\mathbb{N}(\varrho)$ acts as z in the general quadratic equation and values a, b and c in Eq. (59) are obtained as:

$$a = \frac{1}{2}\left[1 + \left[\frac{\partial e(\varrho)}{\partial\mathbb{N}(\varrho)}\right]^2\right], b = \left[\mathbb{N}(\varrho) + e(\varrho)\left[\frac{\partial e(\varrho)}{\partial\mathbb{N}(\varrho)}\right]\right]$$
$$\text{and } c = \frac{\delta}{2}$$
$$(61)$$

To have a single unique of quadratic equation, term $\sqrt{b^2 - 4ac}$ must be equal zero, so, putting values of a, b and c in $\sqrt{b^2 - 4ac} = 0$, we get the value of δ as:

$$\delta = \frac{\left[\mathbb{N}(\varrho) + e(\varrho)\left[\frac{\partial e(\varrho)}{\partial\mathbb{N}(\varrho)}\right]\right]^2}{1 + \left[\frac{\partial e(\varrho)}{\partial\mathbb{N}(\varrho)}\right]^2} \quad (62)$$

Since $\delta \geq 0$, which means

$$\frac{\left[\mathbb{N}(\varrho) + e(\varrho)\left[\frac{\partial e(\varrho)}{\partial\mathbb{N}(\varrho)}\right]\right]^2}{1 + \left[\frac{\partial e(\varrho)}{\partial\mathbb{N}(\varrho)}\right]^2} \geq 0 \quad (63)$$

Therefore, the unique root of Eq. (59) will be given as:

$$\Delta\mathbb{N}(\varrho) = -\frac{b}{2a} = -\frac{\left\{\mathbb{N}(\varrho) + e(\varrho)\left[\frac{\partial e(\varrho)}{\partial\mathbb{N}(\varrho)}\right]\right\}}{1 + \left[\frac{\partial e(\varrho)}{\partial\mathbb{N}(\varrho)}\right]^2} \quad (64)$$

So, Eq. (51) is proved. By substituting Eq. (64) to Eq. (47), we get the following generalized form of the weight update equation:

$$\mathbb{N}(\varrho + 1) = \mathbb{N}(\varrho) + \eta\frac{\left\{\mathbb{N}(\varrho) + e(\varrho)\left[\frac{\partial e(\varrho)}{\partial\mathbb{N}(\varrho)}\right]\right\}}{1 + \left[\frac{\partial e(\varrho)}{\partial\mathbb{N}(\varrho)}\right]^2} \quad (65)$$

The following algorithm shows the pseudo-code for the proposed controller.

Algorithm 1 The proposed SMC-DRNN Pseudo Code

```
Initialize all the weight vectors; W_d^I, W_d^D and W_d^O for the DRNN.
Define all the system parameters according to Eq. (4).
For k = 1: N
    Define the set-point.
    Calculate the error e(t) = x_d1 − x_a1.
    Calculate the equivalent control part u_eq−DRNN(t) using Eq. (39).
    Calculate the sliding surface S(t) using Eq. (40).
    Calculate the switching control term u_sw−DRNN(t) using Eq. (43).
    Calculate the total control law using Eq. (44).
    Calculate the level of the tank (measured output) using Eq. (4).
    Update the weight of DRNN using Eq. (65).
End for
```

6 Simulation results

The developed SMC-DRNN is applied to the nonlinear coupled tank system in this section. To show the robustness of the developed SMC-DRNN, the simulation results of the proposed scheme are compared with other existing schemes such as an adaptive radial basis function neural network estimator-based SMC (ARBFNNE-SMC) [9], which used RBFNN to estimate the dynamics of the controlled system and a PID sliding mode control (PID-SMC), which is designed previously for a coupled tank system [32]. The comparisons are done by measuring some performance indices for all controller such as the mean absolute error (MAE) and the root mean square error (RMSE), which are defined as [34, 35]:
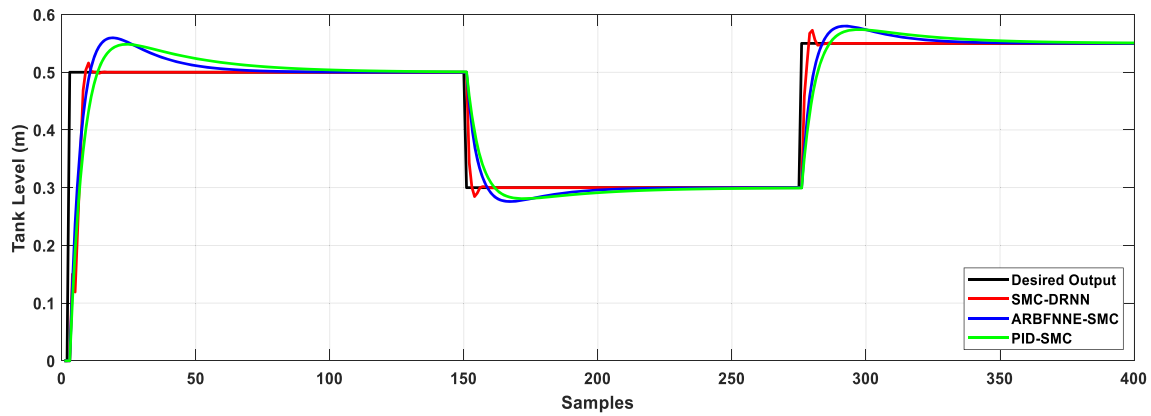
Fig. 5 Response of the coupled-tank system for task 1

$$MAE = \frac{1}{N}\sum_{\varrho=1}^{N}|e(\varrho)| \tag{66}$$

$$RMSE = \sqrt{\frac{1}{N}\sum_{\varrho=1}^{N}e(\varrho)^2} \tag{67}$$

where N is the total number of iterations.

6.1 Task 1: Normal case

In this task, the performance of the coupled-tank system under three different set-points, namely 0.5 m, 0.3 m, and 0.55 m is presented. Figure 5 indicates the output response for the proposed SMC-DRNN, ARBFNNE-SMC and PID-SMC. The performance of the developed SMC-DRNN is better than other schemes in which it has less settling time and overshoot than other controllers. Figure 6 indicates the MAE for all schemes. The MAE for the developed SMC-DRNN is less than those obtained for other schemes. So, the developed SMC-DRNN scheme can track the change of

desired output with good performance compared with other schemes.

6.2 Task 2: Uncertainty due to an external disturbance

This task aims to demonstrate how the uncertainty resulting from external disturbance in the water level of the destination tank affects the coupled-tank system. Figure 7 depicts the response of the system with adding external disturbance; $\Delta L_1 = 0.02$m after at $\varrho = 150$ of simulation. The results indicate that the developed SMC-DRNN has a better performance with less settling time and an overshoot after adding the disturbance value compared with other schemes. Additionally, Fig. 8 displays that the MAE for the developed SMC-DRNN is less than those obtained with other controllers. Therefore, the developed SMC-DRNN can handle the effect of uncertainties due to an external disturbance.
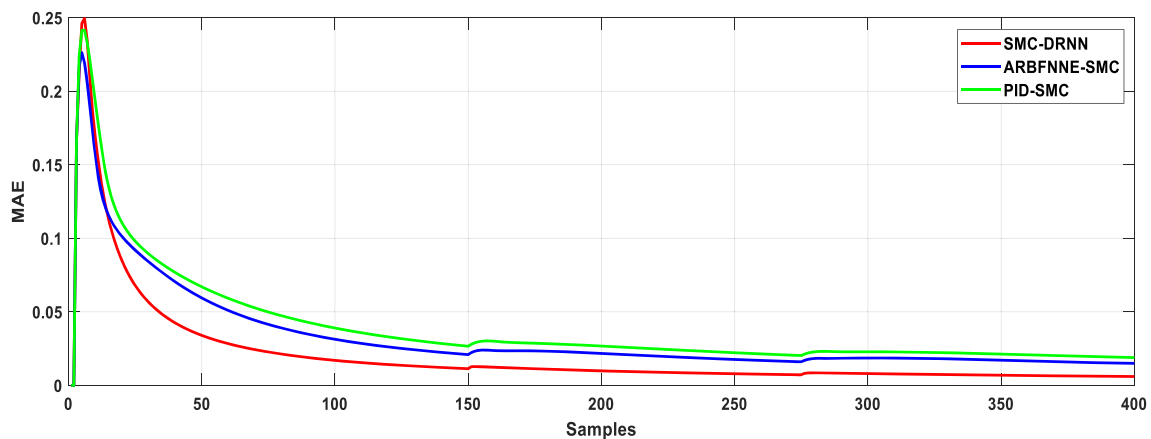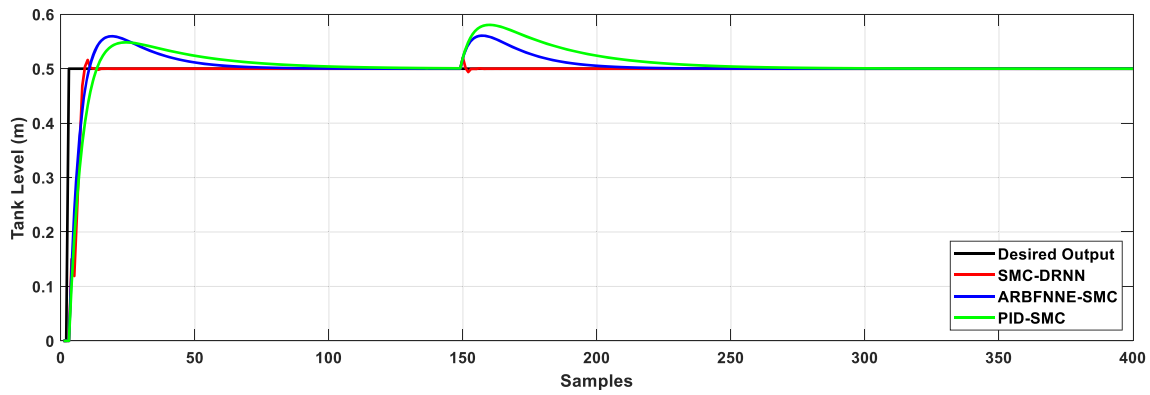

Fig. 6 MAE for task 1

Fig. 7 Response of the coupled-tank system for task 2
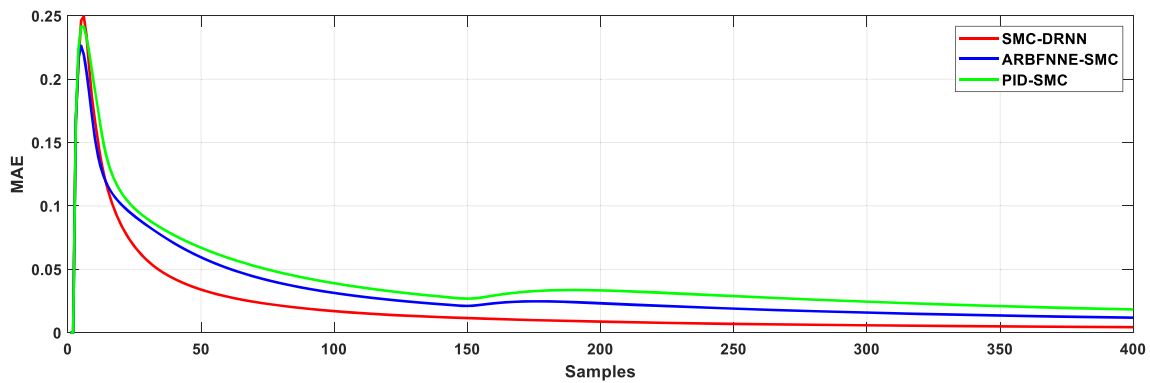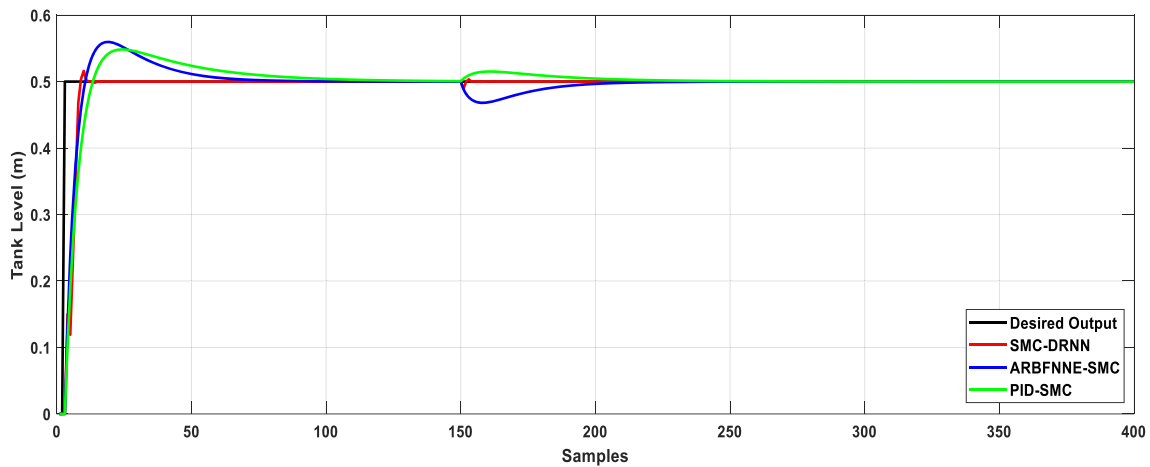

Fig. 8 MAE for task 2

Fig. 9 Response of the coupled-tank system for task 3

6.3 Task 3: Uncertainty in the system parameters

This task demonstrates how introducing uncertainty in the system parameters; A_d and C_2 affects the performance of the system. Figure 9 shows the output of the coupled-tank system when the uncertainty values; $A_d = 0.01$ and $C_2 =$

0.15 are added at $\varrho = 150$ of simulation. Figure 10 shows the MAE for the developed SMC-DRNN and other schemes. It is seen from the results that the developed SMC-DRNN can handle the effect of the uncertainties due to the variations in system parameters compared to other controllers.
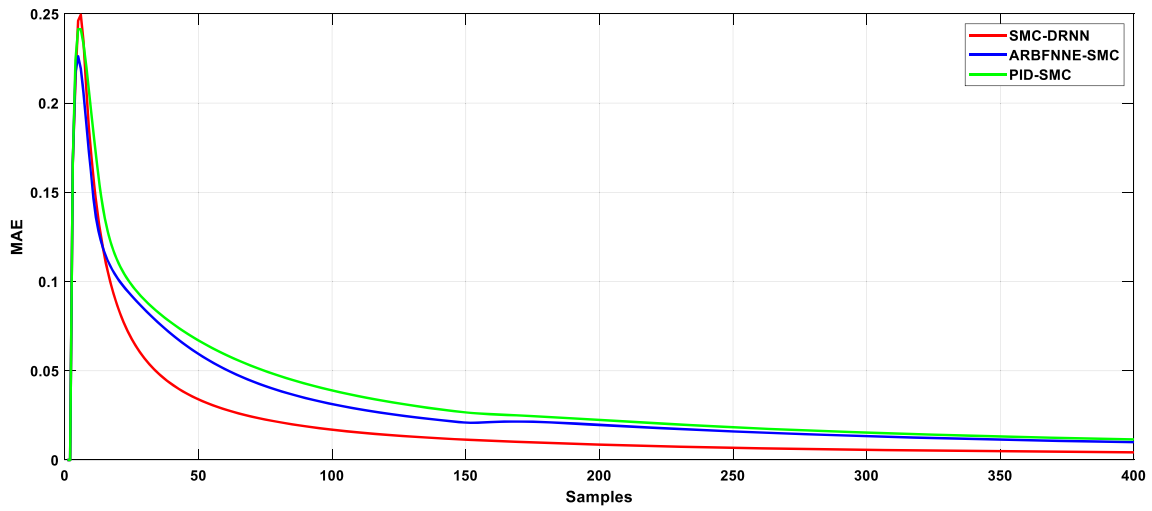
Fig. 10 MAE for task 3
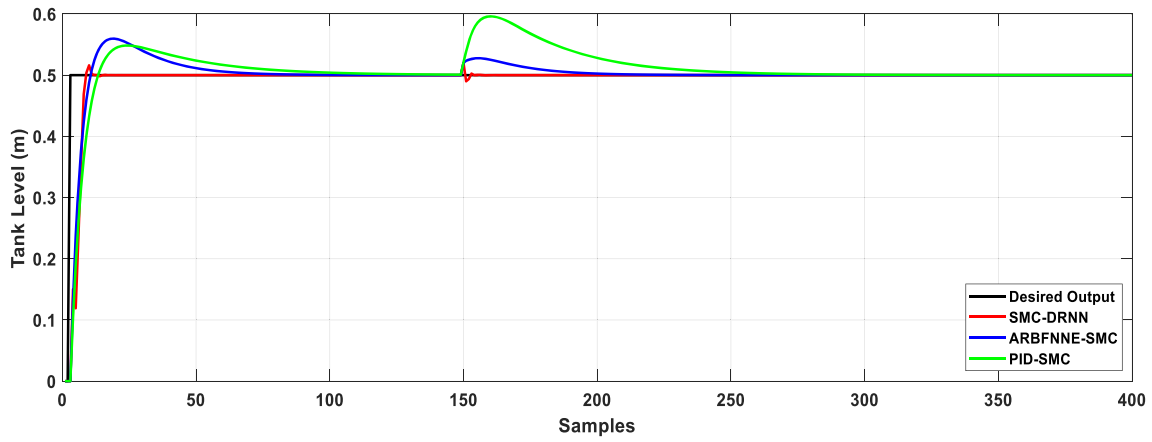
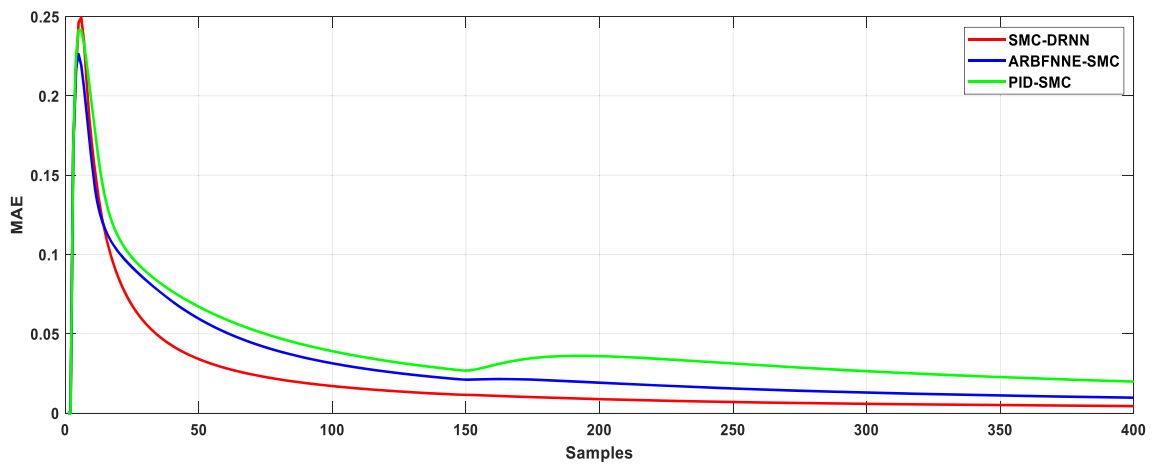**Fig. 11** Response of the coupled-tank system for task 4

Fig. 12 MAE for task 4

6.4 Task 4: Uncertainty due to external disturbance and parameters variations

This task demonstrates the impact of introducing uncertainty in the system parameters; A_d and C_2, as well as the uncertainty resulting from adding external disturbance in the destination tank level. Figure 11 indicates the response of the system after adding uncertainties values; $A_d = 0.01$, $C_2 = 0.15$ and $\Delta L_1 = 0.02m$ at $\varrho = 150$ of simulation. The results indicate that the performance of the developed SMC-DRNN after adding the uncertainty values is better than other controllers in which the settling time and the overshoot for the developed controller are less than those obtained for other schemes. On the other hand, the MAE for the developed SMC-DRNN is less than other schemes as shown in Fig. 12. So, the developed SMC-DRNN can reduce the effect of uncertainties due to the variations in system parameters and external disturbance compared with other controllers.

6.5 Task 5: Uncertainty due to external noise

This task demonstrates the performance of the proposed SMC-DRNN under the effect of uncertainty due to applying random external noise on the system output. Figure 13 shows the system output for the proposed SMC-DRNN and other controllers. Figure 14 shows the MAE for all controllers. The MAE for the proposed SMC-DRNN is less than other controllers. Therefore, the proposed SMC-DRNN can reduce the effect of external random noise.

Tables 2 and 3 present the MAE and RMSE values, respectively, for the proposed SMC-DRNN and other existing schemes; ARBFNNE-SMC [9] and PID-SMC [32]. It is clear that the MAE and RMSE values for the developed SMC-DRNN are less than those obtained for

ARBFNNE-SMC [9] and PID-SMC [32] for all simulation tasks. Therefore, the robustness of the developed SMC-DRNN is better than ARBFNNE-SMC [9] and PID-SMC [32] to handle the effect of system uncertainties due to variations of the system parameters, external disturbance and external random noise.

Table 4 lists the computation time and space complexity of the proposed SMC-DRNN algorithm and other compared algorithms in terms of sliding surface, equivalent control part and sliding surface parameters. It is clear that the computation time for the proposed SMC-DRNN controller is approximately equals the computation time for the ARBFNNE-SMC [9]. The proposed SMC-DRNN uses nonlinear sliding surface, which is designed based on DRNN while the other controllers use linear sliding surface. The proposed SMC-DRNN uses the DRNN to represent the equivalent control part. On the other hand, the ARBFNNE-SMC [9] uses an ARBFNN to represent the equivalent control.

7 Conclusions

In this paper, SMC based-DRNN is introduced for uncertain nonlinear coupled tank system. The control law for the developed scheme consists of two items; the first item is the equivalent control term, which is performed using the DRNN to approximate the dynamics of the coupled tank system. So, the problem of obtaining the precise mathematical model for the controlled process to design the SMC is compensated. The other part of the control law for the developed scheme is the switching control term, in which the sliding surface is performed using the DRNN. The discontinuous signum function is used for the switching control term. Therefore, the problem of chattering is
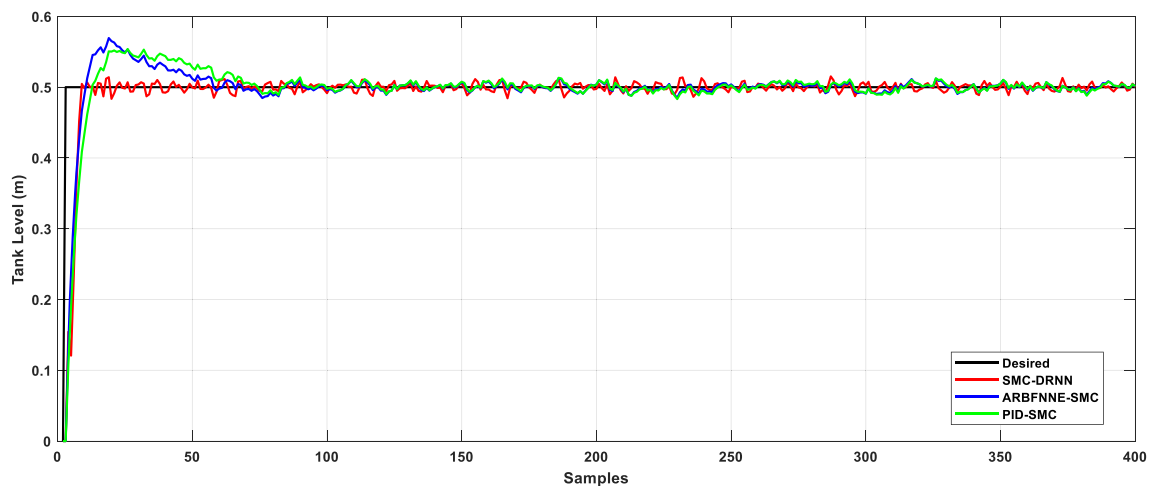

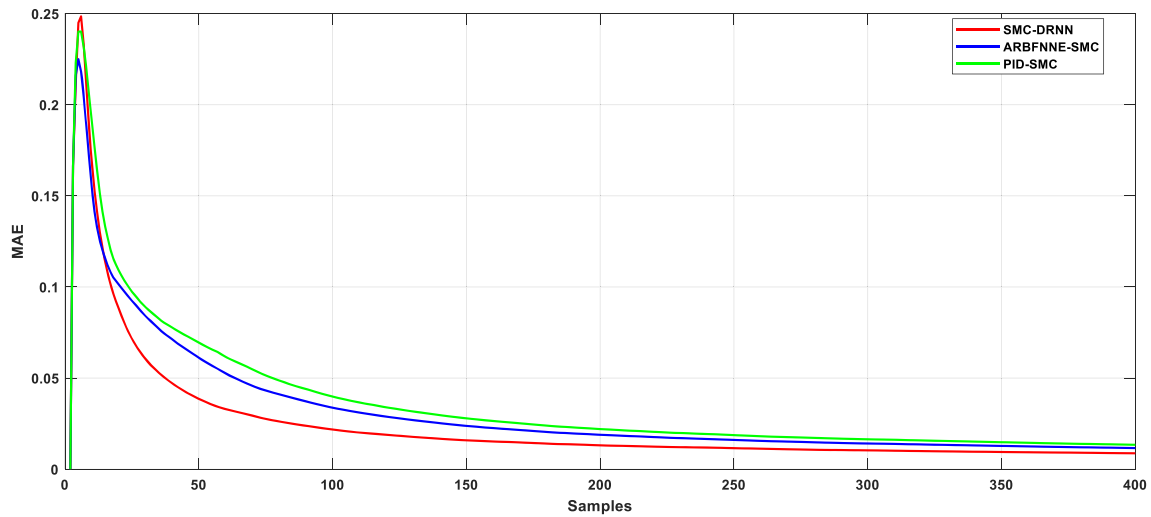**Fig. 13** Response of the coupled-tank system for task 5

Fig. 14 MAE for task 5

Table 2 MAE values for all controllers

	Task 1	Task 2	Task 3	Task 4	Task 5
PID-SMC [32]	0.0189	0.0183	0.0115	0.0198	0.5353
ARBFNNE-SMC [9]	0.0150	0.0118	0.0100	0.0097	0.4634
Proposed SMC-DRNN	0.0060	0.0043	0.0043	0.0043	0.3487

Table 3 RMSE values for all controllers

	Task 1	Task 2	Task 3	Task 4	Task 5
PID-SMC [32]	0.0494	0.0463	0.0417	0.0481	1.678
ARBFNNE-SMC [9]	0.0450	0.0399	0.0384	0.0383	1.573
Proposed SMC-DRNN	0.0426	0.0391	0.0381	0.0380	1.520

compensated. The updating weights of the DRNN are obtained using Lyapunov function to guarantee the controlled system stability. The simulation results including the system uncertainties due to the effect of variations of system parameters and an external disturbance for the proposed controller are compared with other existing schemes to show the robustness of the developed scheme. The compressions are done by measuring the MAE and RMSE for the developed SMC-DRNN and other schemes. The simulation results indicate that the proposed controller can handle the effects of system uncertainties and external disturbances compared to other existing schemes.

Finaly, the proposed SMC-DRNN improved the performance of the controlled system, and it can handle the problem of knowing the perfect mathematical model of the controlled process by using DRNN, which is used to represent the equivalent control part. Also, the proposed controller handles the problem of the chattering by using DRNN to represent the sliding surface and discontinuous signum function. On the other hand, the author uses a constant number of neurons in the hidden layer of DRNN. The performance of the DRNN depends on the number of neurons in the hidden layer and the structure of the network. Therefore, in the future work, the author will develop

Table 4 The time and space complexity of all algorithms

	PID-SMC [32]	ARBFNNE-SMC [9]	Proposed SMC-DRNN
Computation time	0.005 s	0.030 s	0.031 s
Sliding surface	Linear sliding surface based on PID sliding surface	Linear sliding surface based on PID sliding surface	Nonlinear sliding surface based on DRNN
Sliding surface parameters	Constant	Constant	Variable based on DRNN
Equivalent control part	It uses the nominal equivalent control part based on the controlled system model	It uses an adaptive radial basis function NN to represent the equivalent control part	It uses DRNN to represent the equivalent control part

the structure of the DRNN by using self-organizing algorithms to learn or update the structure of the DRNN.

Data availability No datasets were generated or analyzed during the current study.

Declarations

Conflict of interest There is no conflict of interest between the authors to publish this manuscript.

References

1. El-Nagar AM (2016) Embedded intelligent adaptive PI controller for an electromechanical system. ISA Trans 64:314–327
2. Khater AA, El-Nagar AM, El-Bardini M, El-Rabaie NM (2019) Online learning of an interval type-2 TSK fuzzy logic controller for nonlinear systems. J Frankl Inst 356(16):9254–9285
3. El-Nagar AM, El-Bardini M (2014) Practical realization for the interval type-2 fuzzy PD+ I controller using a low-cost microcontroller. Arab J Sci Eng 39:6463–6476
4. Shaheen O, El-Nagar AM, El-Bardini M, El-Rabaie NM (2020) Stable adaptive probabilistic Takagi–Sugeno–Kang fuzzy controller for dynamic systems with uncertainties. ISA Trans 98:271–283
5. El-Nagar AM (2019) Practical implementation for stable adaptive interval A2–C0 type-2 TSK fuzzy controller. Soft Comput 23:9585–9603
6. Chenglong D, Fanbiao L, Chunhua Y (2019) An improved homogeneous polynomial approach for adaptive sliding mode control of Markov jump systems with actuator faults. IEEE Trans Automat Control 65:955–969
7. Eker I (2006) Sliding mode control with PID sliding surface and experimental application to an electromechanical plant. ISA Trans 45:109–118
8. Eker İ (2012) Second-order sliding mode control with PI sliding surface and experimental application to an electromechanical plant. Arab J Sci Eng 37:1969–1986
9. Moawad NM, Elawady WM, Sarhan AM (2019) Development of an adaptive radial basis function neural network estimator-based continuous sliding mode control for uncertain nonlinear systems. ISA Trans 87:200–216
10. Shaalan AS, El-Nagar AM, El-Bardini M, Sharaf M (2020) Embedded fuzzy sliding mode control for polymer extrusion process. ISA Trans 103:237–251
11. Moghaddam JJ, Farahani MH, Amanifard N (2011) A neural network-based sliding-mode control for rotating stall and surge in axial compressors. Appl Soft Comput 11(1):1036–1043
12. Cheng NB, Guan LW, Wang LP, Han J (2011) Chattering reduction of sliding mode control by adopting nonlinear saturation function. Adv Mater Res 143:53–61
13. Tseng ML, Chen MS (2010) Chattering reduction of sliding mode control by low pass filtering the control signal. Asian J Control 12:392–398
14. Yu H, Lloyd S (1997) Variable structure adaptive control of robot manipulators. IEE Proc-Control Theory Appl 144(2):167–176
15. Yau HT, Chen CL (2006) Chattering-free fuzzy sliding-mode control strategy for uncertain chaotic systems. Chaos Solitons Fractals 30:709–718
16. Yusof R, Rahmanb R, Khalida M, Ibrahim M (2011) Optimization of fuzzy model using genetic algorithm for process control application. J Frankl Inst B 348(7):1717–1737
17. Jianxing L et al (2019) Event-triggering dissipative control of switched stochastic systems via sliding mode. Automatica 103:261–273
18. Wu L, Mazumder SK, Kaynak O (2018) Sliding mode control and observation for complex industrial systems—part II. IEEE Trans Ind Electron 65:830–833
19. Su CY, Leung TP (1993) A sliding mode controller with bound estimation for robot manipulators. IEEE Trans Robot Autom 9(2):208–214
20. Yu X, Kaynak O (2009) Sliding-mode control with soft computing: A survey. IEEE Trans Ind Electron 56:3275–3285
21. Hsu C (2013) Adaptive neural complementary sliding-mode control via functional linked wavelet neural network. Eng Appl Artif Intell 26(4):1221–1229
22. Liu H, Zhang T (2012) Adaptive neural network finite-time control for uncertain robotic manipulators. J Intell Robot Syst 134(6):1–15
23. Huang S, Huang K, Chiou K (2003) Development and application of a novel radial basis function sliding mode controller. Mechatronics 13:313–329
24. Sun T, Pei H, Pan Y, Zhou H, Zhang C (2011) Neural network-based sliding mode adaptive control for robot manipulators. Neurocomputing 74(14):2377–2384
25. Yang M, Sheng Z, Yin G, Wang H (2022) A recurrent neural network based fuzzy sliding mode control for 4-DOF ROV movements. Ocean Eng 256:111509
26. Zhao Z, Jin X (2022) Adaptive neural network-based sliding mode tracking control for agricultural quadrotor with variable payload. Comput Electr Eng 103:108336
27. Razmi H, Afshinfar S (2019) Neural network-based adaptive sliding mode control design for position and attitude control of a quadrotor UAV. Aerosp Sci Technol 91:12–27
28. Xia R, Chen M, Wu Q, Wang Y (2020) Neural network based integral sliding mode optimal flight control of near space hypersonic vehicle. Neurocomputing 379:41–52

29. Jiang T, Yan Y, Wu D, Yu S, Li T (2022) Neural network based adaptive sliding mode tracking control of autonomous surface vehicles with input quantization and saturation. Ocean Eng 265:112505

30. Elkenawy A, El-Nagar AM, El-Bardini M, El-Rabaie NM (2020) Diagonal recurrent neural network observer-based adaptive control for unknown nonlinear systems. Trans Inst Meas Control 42(15):2833–2856

31. Kumar R, Srivastava S, Gupta JRP, Mohindru A (2018) Diagonal recurrent neural network based identification of nonlinear dynamical systems with Lyapunov stability based adaptive learning rates. Neurocomputing 287:102–117

32. Ahmed RHIF, Kardous Z, Braie KNB (2012) A PID sliding mode control design for a coupled tank. In: International conference CRATT, pp 1–6

33. El-Nagar AM, El-Bardini M (2014) Derivation and stability analysis of the analytical structures of the interval type-2 fuzzy PID controller. Appl Soft Comput 24:704–716

34. Khater AA, El-Nagar AM, El-Bardini M, El-Rabaie NM (2020) Online learning based on adaptive learning rate for a class of recurrent fuzzy neural network. Neural Comput Appl 32:8691–8710

35. Zaki AM, El-Nagar AM, El-Bardini M, Soliman FAS (2021) Deep learning controller for nonlinear system based on Lyapunov stability criterion. Neural Comput Appl 33:1515–1531